On the Physical Nature of Zonal Jet EOFs

Adam Hugh Monahan[1,2] and John C. Fyfe[3]

[1] School of Earth and Ocean Sciences
University of Victoria, Victoria, BC, Canada
(email: monahana@uvic.ca)

[2] Earth System Evolution Program
Canadian Institute for Advanced Research, Toronto, ON, Canada

[3] Canadian Centre for Climate Modelling and Analysis
Meteorological Service of Canada
University of Victoria, Victoria, BC, Canada
(email: John.Fyfe@ec.gc.ca)

Submitted to Journal of Climate

November 24, 2005

Abstract

Analytic results are obtained for the mean and covariance structure of an idealised zonal jet which fluctuates in strength, position, and width. Through a systematic perturbation analysis, the leading Empirical Orthogonal Functions (EOFs) and Principal Component (PC) time series are obtained. These EOFs are built up of linear combinations of basic patterns corresponding to monopole, dipole, and tripole structures. The analytic results demonstrate that in general the individual EOF modes cannot be interpreted in terms of individual physical processes. In particular, while the dipole EOF (similar to the leading EOF of the midlatitude zonal mean zonal wind) describes fluctuations in jet position to leading order, its time series also contains contributions from fluctuations in strength and width. No simple interpretations of the other EOFs in terms of strength, position, or width fluctuations are possible. Implications of these results for the use of EOF analysis to diagnose physical processes of variability are discussed.

1 Introduction

Empirical Orthogonal Function (EOF) analysis, also known as Principal Component Analysis (PCA), is a standard technique for decomposing an observed geophysical field into a set of orthogonal spatial patterns with associated temporally uncorrelated time series. These spatial patterns (denoted the EOFs), are obtained as the eigenvectors of the covariance matrix of the field, while the time series (denoted the principal components, or PCs) arise as the projection coefficients of the corresponding EOF pattern on the original field. It is common to interpret individual EOF/PC pairs (together referred to as a mode) as corresponding to distinct physical processes, where the term *physical process* is used to denote a degree of freedom of the system with a clear physical interpretation. It was emphasized by North (1984), however, that individual EOF modes correspond to individual physical modes only in a very limited class of physical systems (those governed by linear dynamics for which the linear operator commutes with its adjoint). In general, observed geophysical flows do not belong to this class of systems (e.g. Farrell and Ioannou, 1996; Penland, 1996; Palmer, 1999). In particular, if the underlying physical processes are localised, nonstationary, not mutually orthogonal, or nonlinearly coupled, they will generally be spread across a number of EOF modes (e.g. Ambaum et al., 2001; Dommenget and Latif, 2002; Fyfe, 2003; Monahan et al., 2003; Fyfe and Lorenz, 2005). Individual EOF modes cannot in general be expected to correspond to individual physical processes.

In particular, EOF analysis has been used to study the low-frequency (10-100 days) variability of the extratropical atmosphere (e.g. Barnston and Livezey, 1987; Thompson and Wallace, 2000). In both hemispheres, throughout the troposphere, it is found that the meridional spatial structure of the dominant EOF mode of the zonal mean zonal wind is a dipole centred at approximately the latitude of the core of the time-mean jet. This structure is generally interpreted as representing meridional displacements of the eddy-driven jet (the

so-called zonal index), while higher order EOFs are interpreted as reflecting changes in jet strength or width (e.g. Feldstein and Lee, 1998; Feldstein, 2000; DeWeaver and Nigam, 2000; Codron, 2005; Vallis et al., 2004). Wittman et al. (2005) consider numerical simulations of the EOF structure of an idealised midlatitude zonal jet (as in Fyfe (2003) and Fyfe and Lorenz (2005)) characterised by Gaussian fluctuations in strength, position, and width (denoted respectively pulsing, wobbling, and bulging). It is shown that a meridional dipole arises as the leading EOF of pure wobbling motion, and that neither pulsing nor bulging (both of which are symmetric about the jet axis) produce dipole EOF patterns (which are asymmetric about the jet axis). A meridional dipole was also found in the study of Gerber and Vallis (2005) as the leading EOF of a one-dimensional spatially stochastic process that conserves angular momentum.

The present study takes as its starting point the idealised midlatitude jet considered in Wittman et al. (2005), and obtains analytic expressions for the EOFs and PCs in terms of the fluctuations in jet strength, position, and width. These analytic results allow unambiguous diagnoses of the relationships between the EOF modes and the underlying physical processes. It will be shown that while the leading EOFs are made up of a small number of basic spatial patterns, and are therefore simple in structure, the associated time series inextricably couple the underlying processes of jet variability. Furthermore, because the EOFs associated with one physical process are not orthogonal to those associated with another, these EOFs will be seen to be mixed when both processes are present simultaneously. It will be shown that in this idealised (but physically motivated) system, while some EOF modes may be associated with individual physical processes to a leading order approximation, this association cannot generally be made. The present study differs from earlier studies demonstrating difficulties in associating individual physical processes with individual EOF modes (e.g. Ambaum et al., 2001; Dommenget and Latif, 2002) in its use of a physically motivated system: the fluctuating zonal jet.

Section 2 describes the idealised fluctuating midlatitude jet considered in this study. The EOFs of the jet in the case of pure fluctuations in strength, position, and width are considered respectively in Sections 3, 4 and 5. Section 6 describes the covariance structure in the presence of simultaneous fluctuations in both strength and position, while the case of correlated fluctuations in strength and width is considered in Section 7. The EOF structure for simultaneous fluctuations in strength, position, and width is discussed in Section 8. A discussion and conclusions are presented in Section 9.

2 The Idealised Gaussian Jet

Following Fyfe (2003), Fyfe and Lorenz (2005), and Wittman et al. (2005) we consider our fundamental dynamical object to be a jet in the zonal mean zonal wind with a simple Gaussian profile:

$$u(\phi, t) = U(t) \exp\left(-\frac{(\phi - \Phi(t))^2}{2\sigma^2(t)}\right), \tag{1}$$

where the $U(t)$, $\Phi(t)$ and $\sigma(t)$ are the jet strength, position and width, respectively. We proceed to investigate the statistical structure of $u(\phi, t)$ by assuming

$$U(t) = U_0 + \xi(t) \tag{2}$$

$$\Phi(t) = \phi_0 + \lambda(t) \tag{3}$$

$$\sigma^{-1}(t) = \sigma_0^{-1}(1 + \eta(t)), \tag{4}$$

where $\xi(t)$, $\lambda(t)$, and $\eta(t)$ are individually Gaussian time series with mean zero, i.e.,

$$p(\xi) = \frac{1}{\sqrt{2\pi\gamma^2}} \exp\left(-\frac{\xi^2}{2\gamma^2}\right) \tag{5}$$

$$p(\lambda) = \frac{1}{\sqrt{2\pi w^2}} \exp\left(-\frac{\lambda^2}{2w^2}\right) \tag{6}$$

$$p(\eta) = \frac{1}{\sqrt{2\pi v^2}} \exp\left(-\frac{\eta^2}{2v^2}\right). \tag{7}$$

For the purposes of calculating means and covariances of the zonal wind, the temporal autocorrelation structures of these time series are irrelevant. Note that the expression for the inverse width (Eqn. (4)) allows σ to become negative, which is of course unphysical; in practice, the standard deviation of η is sufficiently small that the probability of negative values of the jet width is negligible.

Observational justification for these approximations is provided in Figure 1, the top panel of which shows the leading EOFs of daily Southern Hemisphere winter (May-Sep.) 500 hPa zonal mean zonal wind after fitting to the profile (1) (following the direct procedure in Appendix B) and then reconstructing $\lambda(t)$ and $\eta(t)$ to be individually Gaussian with observed variances. Additionally, in order to preserve the observed correlation between strength and inverse width, we set $\xi(t) = \rho\eta(t)$. As discussed in Fyfe and Lorenz (2005), the observed correlation between strength and inverse width reflects conservation of angular momentum:

$$M(t) = \int_{-\infty}^{\infty} u(\phi, t) d\phi = \sqrt{2\pi}\sigma_0 \frac{U_0 + \xi(t)}{1 + \eta(t)} \tag{8}$$

(where the sphericity of the domain has been neglected). We note that there is no manifest dependence between either strength and position or width and position. Of course, angular momentum conservation on a spherical domain implies that poleward (equatorward) displacements of the jet should be associated with increased (decreased) jet strength; the lack of correlation between $U(t)$ and $\Phi(t)$ indicates that this relationship is weaker than that between $U(t)$ and $\sigma(t)$. Under these assumptions the system is completely described in terms of the following best fit parameters: $U_0 \approx 23.3$ m s^{-1}, $\gamma \approx 2.7$ m s^{-1}, $\phi_0 \approx -47.5$ deg, $w \approx 2.7$ deg, $\sigma_0^{-1} \approx 0.095$ deg^{-1}, $v \approx 0.165$ and $\rho \approx 13.1$ m s^{-1}. We now compare the leading EOFs obtained in this way with the leading EOFs of the unfit zonal mean zonal winds (Figure 1, bottom). We see that despite all the rather stringent approximations imposed by (1)-(7) the two sets of leading EOFs compare very well: the idealised model does a good job of capturing the mean and covariance structure of the original data.

Having specified the statistical structure of the fluctuations in jet strength, position, and width, we can calculate the time mean of $u(\phi,t)$:

$$\langle u(\phi)\rangle = \int p(\xi,\lambda,\eta)(U_0+\xi)\exp\left(-\frac{(\phi-\phi_0-\lambda)^2(1+\eta)^2}{2\sigma_0^2}\right)d\xi d\lambda d\eta, \tag{9}$$

and the spatial covariance function of $u(\phi,t)$:

$$C(\phi_1,\phi_2) = \langle u(\phi_1)u(\phi_2)\rangle - \langle u(\phi_1)\rangle\langle u(\phi_2)\rangle\,, \tag{10}$$

where the angle brackets $\langle\cdot\rangle$ denote the expectation (or averaging) operator (and we use the simplified notation $\langle u(\phi)\rangle = \langle u(\phi,t)\rangle$). Once the covariance function has been calculated, the eigenvalue problem for the EOFs can be posed as an integral equation as described in Appendix A. For the analysis of $C(\phi_1,\phi_2)$ which follows it is useful to define the functions:

$$f_0(\phi) = \left(\frac{1}{\sqrt{\pi}\sigma_0}\right)^{1/2}\exp\left(-\frac{(\phi-\phi_0)^2}{2\sigma_0^2}\right) \tag{11}$$

$$f_1(\phi) = \left(\frac{1}{\sqrt{\pi}\sigma_0}\right)^{1/2}H_1\left(\frac{(\phi-\phi_0)}{\sqrt{2}\sigma_0}\right)\exp\left(-\frac{(\phi-\phi_0)^2}{2\sigma_0^2}\right) \tag{12}$$

$$f_2(\phi) = \left(\frac{1}{3\sqrt{\pi}\sigma_0}\right)^{1/2}H_2\left(\frac{(\phi-\phi_0)}{\sqrt{2}\sigma_0}\right)\exp\left(-\frac{(\phi-\phi_0)^2}{2\sigma_0^2}\right), \tag{13}$$

where $H_1(x) = 2x$ and $H_2(x) = 4x^2-2$ are the Hermite polynomials of order 1 and 2 (Arfken, 1985). The functions $f_i(\phi)$ are normalised to have unit square norm: $\int_{-\infty}^{\infty} f_i^2(\phi)\,d\phi = 1\ ,\ i = 0,1,2$. Plots of these functions are given in Figure 2. It is worth noting that despite their resemblance to parabolic cylinder functions (e.g. Gill, 1982), these functions are not mutually orthogonal. By symmetry, $f_1(\phi)$ is orthogonal to both $f_0(\phi)$ and $f_2(\phi)$ but $f_0(\phi)$ and $f_2(\phi)$ are not mutually orthogonal, i.e. $\int_{-\infty}^{\infty} f_0(\phi)f_2(\phi)\,d\phi = -1/\sqrt{3}$. Figure 3 provides a geometric representation of the vector space spanned by these functions.

We now proceed to develop analytic expressions for the covariance function and EOFs of the fluctuating jet for progressively complex forms of variability: first, individual fluctuations in strength, position, and width; and second, simultaneous fluctuations in strength and position, and in strength and width. While these individual examples do not describe the

full covariance structure of the fully variable jet, they represent important limiting cases which can be used to understand the more complex case. In this analysis, the sphericity of the earth will be neglected: the jet will be taken to exist on an infinite domain.

3 Fluctuations in Jet Strength Alone

Consider first the case in which only fluctuations in strength are nonzero (i.e. $\gamma \neq 0$, $w = 0$, $v = 0$). The time mean jet is:

$$\begin{aligned} \langle u(\phi) \rangle &= \int_{-\infty}^{\infty} p(\xi)(U_0 + \xi) \exp\left(-\frac{(\phi - \phi_0)^2}{2\sigma_0^2}\right) \, d\xi \\ &= U_0 \exp\left(-\frac{(\phi - \phi_0)^2}{2\sigma_0^2}\right). \end{aligned} \tag{14}$$

In this case the time mean jet is identical to the instantaneous jet with time mean strength. The covariance function is

$$C(\phi_1, \phi_2) = \gamma^2 \exp\left(-\frac{(\phi_1 - \phi_0)^2}{2\sigma_0^2}\right) \exp\left(-\frac{(\phi_2 - \phi_0)^2}{2\sigma_0^2}\right) \tag{15}$$

$$= \sqrt{\pi}\sigma_0\gamma^2 f_0(\phi_1) f_0(\phi_2). \tag{16}$$

Thus, the integral equation defining the eigenvalue problem for the EOFs (67) is characterised by a kernel that is trivially separable in the function $f_0(\phi)$, which is therefore the only eigenfunction associated with a nonzero eigenvalue (Arfken, 1985). In the presence of Gaussian fluctuations in the jet strength alone, the leading (and only) EOF is the monopole

$$E^{(1)}(\phi) = f_0(\phi). \tag{17}$$

Note that this provides an analytic demonstration of the result found numerically in Wittman et al. (2005).

4 Fluctuations in Jet Position Alone

Now consider the case in which only fluctuations in jet position are nonzero (i.e. $\gamma = 0$, $w \neq 0$, $v = 0$). The time mean jet is:

$$\begin{aligned} \langle u(\phi) \rangle &= \int_{-\infty}^{\infty} p(\lambda) U_0 \exp\left(-\frac{((\phi - \phi_0) - \lambda)^2}{2\sigma_0^2} \right) d\lambda \\ &= \frac{U_0 \sigma_0}{\sqrt{\sigma_0^2 + w^2}} \exp\left(-\frac{(\phi - \phi_0)^2}{2(\sigma_0^2 + w^2)} \right). \end{aligned} \tag{18}$$

In this case the time mean jet differs from the instantaneous jet at the time mean position. In particular, the jet wobbling around its mean position produces a mean jet that is weaker and wider than the instantaneous jet at the mean position. The covariance function is

$$\begin{aligned} C(x,y) &= \frac{U_0^2 \sigma_0}{\sqrt{\sigma_0^2 + 2w^2}} \exp\left(-\frac{\sigma_0^2 + w^2}{\sigma_0^2 + 2w^2}(x^2 + y^2) \right) \exp\left(\frac{2w^2}{\sigma_0^2 + 2w^2} xy \right) \\ &\quad - \frac{U_0^2 \sigma_0^2}{\sigma_0^2 + w^2} \exp\left(-\frac{\sigma_0^2}{\sigma_0^2 + w^2}(x^2 + y^2) \right), \end{aligned} \tag{19}$$

where we have defined the new coordinates

$$x = \frac{\phi_1 - \phi_0}{\sqrt{2}\sigma_0} \tag{20}$$

$$y = \frac{\phi_2 - \phi_0}{\sqrt{2}\sigma_0}. \tag{21}$$

Defining the parameter $h = w/\sigma_0$ the covariance function can be expressed

$$\begin{aligned} C(x,y) &= \frac{U_0^2}{\sqrt{1 + 2h^2}} \exp\left(-\frac{1 + h^2}{1 + 2h^2}(x^2 + y^2) \right) \\ &\quad \times \left[\exp\left(\frac{2h^2}{1 + 2h^2} xy \right) - \frac{\sqrt{1 + 2h^2}}{1 + h^2} \exp\left(\frac{h^4}{(1 + h^2)(1 + 2h^2)}(x^2 + y^2) \right) \right]. \end{aligned} \tag{22}$$

This covariance function is not obviously separable for general values of h. However, in the limit of small fluctuations in position ($h << 1$), expanding the quantity in square brackets in (22) in powers of h yields:

$$C(x,y) = U_0^2 e^{-(x^2+y^2)} \left[\frac{1}{2}(h^2 - 2h^4) H_1(x) H_1(y) + \frac{1}{8} h^4 H_2(x) H_2(y) + O(h^6) \right] (1 + O(h^2)). \tag{23}$$

Changing coordinates back to ϕ_1, ϕ_2, the covariance function can be written in the manifestly separable form:

$$C(\phi_1, \phi_2) = \frac{\sqrt{\pi}\sigma_0 U_0^2}{2}\left[(h^2 - 2h^4) f_1(\phi_1) f_1(\phi_2) + \frac{3}{4}h^4 f_2(\phi_1) f_2(\phi_2) + O(h^6)\right](1+O(h^2)). \quad (24)$$

As discussed in Appendix A, because the functions $f_1(\phi)$ and $f_2(\phi)$ are mutually orthogonal, it follows that these functions are also EOFs. Furthermore, the ordering of the EOFs is clear from the expansion in powers of h:

$$E^{(1)}(\phi) = f_1(\phi) \quad (25)$$

$$E^{(2)}(\phi) = f_2(\phi). \quad (26)$$

For small fluctuations in jet position (relative to jet width), the first EOF is the dipole $f_1(\phi)$ and the second EOF is the tripole $f_2(\phi)$, precisely in accordance with the numerical results of Wittman et al. (2005).

Having obtained analytic expressions for the EOFs, it is possible to calculate the PC time series:

$$\alpha^{(i)}(t) = \int_{-\infty}^{\infty} E^{(i)}(\phi)(u(\phi, t) - \langle u(\phi)\rangle) d\phi. \quad (27)$$

To leading order, these are respectively

$$\alpha^{(1)}(t) = \left(\frac{\sqrt{\pi}}{2\sigma_0}\right)^{1/2} U_0 \lambda(t) + O(h^2) \quad (28)$$

$$\alpha^{(2)}(t) = \left(\frac{3\sqrt{\pi}}{\sigma_0}\right)^{1/2} \frac{U_0}{4\sigma_0}(\lambda(t)^2 - w^2) + O(h^4). \quad (29)$$

While the PC time series are uncorrelated by construction, $\alpha^{(1)}(t)$ and $\alpha^{(2)}(t)$ are clearly *not* independent: their joint distribution is parabolic. For the problem under consideration, at every time t, the wind field is specified by the single number $\lambda(t)$. Because variations in the jet project on a spectrum of EOFs, the PC of all of these EOFs must be determined uniquely by the scalar time series $\lambda(t)$, and cannot be mutually independent. This result was first obtained by Fyfe and Lorenz (2005) using a Taylor series expansion of the wobbling jet; the above analysis formalizes the argument.

5 Fluctuations in Jet Width Alone

Consider the case in which only fluctuations in jet width are nonzero (i.e. $\gamma = 0$, $w = 0$, $v \neq 0$). The time mean jet is

$$\begin{aligned} \langle u(\phi) \rangle &= \int_{-\infty}^{\infty} p(\eta) U_0 \exp\left(-\frac{(1+\eta)^2}{2\sigma_0^2} (\phi - \phi_0)^2 \right) \, d\eta \\ &= \frac{U_0 \sigma_0}{\sqrt{\sigma_0^2 + v^2(\phi - \phi_0)^2}} \exp\left(-\frac{(\phi - \phi_0)^2}{2(\sigma_0^2 + v^2(\phi - \phi_0)^2)} \right). \end{aligned} \tag{30}$$

As was the case with fluctuations in position, the mean jet is not equal to the instantaneous jet at mean width. The covariance function is

$$\begin{aligned} C(x,y) &= \frac{U_0^2}{\sqrt{(1+v^2x^2)(1+v^2y^2)}} \exp\left(-\frac{x^2+y^2}{2(1+v^2(x^2+y^2))} \right) \\ &\times \left[\sqrt{1 + \frac{v^4 x^2 y^2}{1+v^2(x^2+y^2)}} - \exp\left(-\frac{1}{2} \frac{v^2 x^2 y^2}{1+v^2(x^2+y^2)} \left[\frac{1}{1+v^2x^2} + \frac{1}{1+v^2y^2} \right] \right) \right] \end{aligned} \tag{31}$$

where

$$x = (\phi_1 - \phi_0)/\sigma_0 \tag{32}$$

$$y = (\phi_2 - \phi_0)/\sigma_0. \tag{33}$$

As was the case with fluctuations in position alone, this covariance function is not obviously separable for general values of v. However, for $v << 1$,

$$C(x,y) = \frac{U_0^2}{\sqrt{(1+v^2x^2)(1+v^2y^2)}} \exp\left(-\frac{x^2+y^2}{2(1+v^2(x^2+y^2))} \right) \left(v^2 x^2 y^2 + O(v^4) \right) \tag{34}$$

so to $O(v^4)$,

$$C(\phi_1, \phi_2) = \frac{3\sqrt{\pi}\sigma_0 U_0^2}{4} v^2 \left[f_2(\phi_1) + \frac{2}{\sqrt{3}} f_0(\phi_1) \right] \left[f_2(\phi_2) + \frac{2}{\sqrt{3}} f_0(\phi_2) \right] + O(v^4). \tag{35}$$

The leading EOF for pure fluctuations in jet width is therefore,

$$E^{(1)}(\phi) = f_2(\phi) + \frac{2}{\sqrt{3}} f_0(\phi). \tag{36}$$

This EOF, illustrated in Figure 4, is in excellent agreement with the leading EOF of pure fluctuations in jet width obtained numerically in Wittman et al. (2005).

The orientations in the space spanned by $f_0(\phi)$, $f_1(\phi)$, and $f_2(\phi)$ of the leading EOFs for the cases of pure fluctuations in jet strength, position and width are presented in Figure 5.

6 Independent Fluctuations in Strength and Position

We now turn to the case in which only fluctuations in width are zero (i.e. $\gamma \neq 0, w \neq 0$, $v = 0$), and where, as suggested by the observations, the fluctuations in strength and position are independent, i.e.:

$$p(\xi, \lambda) = p(\xi)p(\lambda) = \frac{1}{2\pi\gamma w} \exp\left(-\frac{\xi^2}{2\gamma^2}\right) \exp\left(-\frac{\lambda^2}{2w^2}\right). \tag{37}$$

Then the time mean jet is:

$$\begin{aligned} \langle u(\phi) \rangle &= \int_{-\infty}^{\infty} \int_{-\infty}^{\infty} (U_0 + \xi) \exp\left(-\frac{((\phi - \phi_0) - \lambda)^2}{2\sigma_0^2}\right) p(\xi, \lambda)\, d\xi\, d\lambda \\ &= \frac{U_0 \sigma_0}{\sqrt{\sigma_0^2 + w^2}} \exp\left(-\frac{(\phi - \phi_0)^2}{2(\sigma_0^2 + w^2)}\right). \end{aligned} \tag{38}$$

Not surprisingly, the mean jet depends on fluctuations in jet position but not in jet strength. Defining the coordinates x and y as in Eqns. (20) and (21), the covariance function is

$$\begin{aligned} C(x, y) &= \frac{U_0^2}{\sqrt{1 + 2h^2}} \exp\left(-\frac{1 + h^2}{1 + 2h^2}(x^2 + y^2)\right) \\ &\quad \times \left[(1 + l^2) \exp\left(\frac{2h^2}{1 + 2h^2} xy\right) - \frac{\sqrt{1 + 2h^2}}{1 + h^2} \exp\left(\frac{h^4}{(1 + h^2)(1 + 2h^2)}(x^2 + y^2)\right)\right] \end{aligned} \tag{39}$$

where $l = \gamma / U_0$. As was the case of fluctuations in jet position alone, this covariance function becomes manifestly separable when we assume that h is small and expand in powers of h:

$$\begin{aligned} C(x, y) &= U_0^2 \exp(-(x^2 + y^2)) \\ &\quad \times \left[l^2 + \frac{1}{2}(h^2 + l^2 h^2 - 2h^4) H_1(x) H_1(y) + \frac{1}{8} h^4 H_2(x) H_2(y) + h.o.t.\right] (1 + O(h^2)) \end{aligned} \tag{40}$$

where we have also assumed that l is "small". Transforming back to the original coordinates we obtain

$$C(\phi_1, \phi_2) = \sqrt{\pi}\sigma_0 U_0^2 \left[l^2 f_0(\phi_1) f_0(\phi_2) + \frac{1}{2}(h^2 + l^2 h^2) f_1(\phi_1) f_1(\phi_2) + \frac{3}{8} h^4 f_2(\phi_1) f_2(\phi_2) \right] + h.o.t. \tag{41}$$

The covariance function is clearly separable in $f_j(\phi)$, $j = 0, 1, 2$. As noted earlier, while $f_1(\phi)$ is orthogonal to both $f_0(\phi)$ and $f_2(\phi)$, $f_0(\phi)$ and $f_2(\phi)$ are not mutually orthogonal. Thus, while $f_1(\phi)$ is one of the three leading EOFs of the covariance function (41), the other two will be orthogonal linear combinations of $f_0(\phi)$ and $f_2(\phi)$:

$$E^{(\pm)}(\phi) = \beta_0^{(\pm)} f_0(\phi) + \beta_2^{(\pm)} f_2(\phi) \tag{42}$$

where the plus (minus) superscript labels the EOF associated with the larger (smaller) variance. The EOF problem can then be recast as a 2-dimensional eigenvalue problem, details of which are given in Appendix A. Figure 6 displays plots of $\beta_0^{(\pm)}$ and $\beta_2^{(\pm)}$ as functions of the ratio $3h^4/8l^2$. For small values of the ratio, that is, for $h^4 << l^2$, $\beta_0^+ \simeq 1$ and $\beta_2^+ \simeq 0$. The EOF $E^{(+)}(\phi)$ is therefore approximately equal to $f_0(\phi)$, the leading EOF for pure fluctuations in jet strength (up to a sign, always arbitrary for EOFs). For large values of the ratio, that is, for $h^4 >> l^2$, $\beta_2^+ \simeq 1$ and $\beta_0^+ \simeq 0$. In this limit, $E^{(+)}(\phi) \simeq f_2(\phi)$, the second EOF for pure fluctuations in jet position. However, for intermediate values of the ratio, $E^{(+)}(\phi)$ is necessarily a mixture of $f_0(\phi)$ and $f_2(\phi)$; that is, is a hybrid structure which does not correspond to an EOF found in either of the cases of pure jet position or strength fluctuations (Figure 7). For all values of the ratio $3h^4/8l^2$, $E^{(-)}(\phi)$ is also a hybrid of the vectors $f_0(\phi)$ and $f_2(\phi)$. Fluctuations in both strength and position are combined inextricably in the structure of the EOFs. The structure of the dipole EOF of jet position variations, on the other hand, is unaffected by fluctuations in the jet strength.

Note that these calculations allow us not only to identify the leading EOFs, but their ordering as well. It is straightforward to show (Appendix A, Eq. (73)) that the ratio of

the variance of the PC time series associated with the eigenvector $E^{(-)}(\phi)$ to that of the eigenvector $f_1(\phi)$ is (at most) of order h^2, so $f_1(\phi)$ is always a higher order EOF than $E^{(-)}(\phi)$. The ordering of $E^{(+)}(\phi)$ relative to $f_1(\phi)$ depends on the relative magnitudes of the variance of the PC corresponding to $E^{(+)}(\phi)$,

$$\mu^{(+)} = \frac{\sqrt{\pi}\sigma_0 U_0^2}{2}\left(l^2 + \frac{3h^4}{8} + \sqrt{\left(l^2 + \frac{3h^4}{8}\right)^2 - l^2h^4}\right) \tag{43}$$

(Appendix A), and that of the PC corresponding to $f_1(\phi)$, $\sqrt{\pi}\sigma_0 U_0^2 h^2/2$:

$$\left\{E^{(1)}(\phi), E^{(2)}(\phi), E^{(3)}(\phi)\right\} = \left\{f_1(\phi), E^{(+)}(\phi), E^{(-)}(\phi)\right\} \quad \text{if} \quad \frac{2\mu^{(+)}}{\sqrt{\pi}\sigma_0 U_0^2} < h^2,$$
$$\left\{E^{(1)}(\phi), E^{(2)}(\phi), E^{(3)}(\phi)\right\} = \left\{E^{(+)}(\phi), f_1(\phi), E^{(-)}(\phi)\right\} \quad \text{if} \quad \frac{2\mu^{(+)}}{\sqrt{\pi}\sigma_0 U_0^2} > h^2.$$

As it is the first of these two cases that is relevant to the midlatitude tropospheric jets, we will assume this ordering for the remainder of this section.

While the spatial pattern of the dipole EOF arising in the case of pure jet position fluctuations is unaffected by the addition of jet strength fluctuations, the associated principal component time series couples both forms of variability:

$$\alpha^{(1)}(t) = \left(\frac{\sqrt{\pi}}{2\sigma_0}\right)^{1/2}(U_0 + \xi(t))\lambda(t) + h.o.t. \tag{44}$$

Variations of $\xi(t)$ change the overall amplitude of $u(\phi, t)$, so they must project on the dipole EOF. Clearly, the time series of the dipole EOF cannot be simply interpreted as reflecting variability in jet position alone (although for relatively weak fluctuations in jet strength the differences will be small).

The interpretation of the second principal component time series, $\alpha^{(2)}(t)$ is even more complicated because $E^{(2)}(\phi)$ is a hybrid of $f_0(\phi)$ and $f_2(\phi)$:

$$\begin{aligned}\alpha^{(2)}(t) &= \beta_0^{(+)}\left(\sqrt{\pi}\sigma_0\right)^{1/2}\left[\xi(t) - \frac{U_0}{4\sigma_0^2}(\lambda^2(t) - w^2) - \frac{\lambda^2(t)\xi(t)}{4\sigma_0^2}\right] \\ &\quad + \beta_2^{(+)}\left(\frac{3\sqrt{\pi}}{\sigma_0}\right)^{1/2}\frac{(U_0 + \xi(t))}{4\sigma_0}(\lambda(t)^2 - w^2) + h.o.t.\end{aligned} \tag{45}$$

Regardless of the degree of alignment of $E^{(2)}(\phi)$ along either $f_0(\phi)$ or $f_2(\phi)$, the PC time series $\alpha^{(2)}$ is an inextricable mixture of variability in both jet strength and position. Only in the limiting cases of $l >> h^2$ and $l << h^2$ can this time series reasonably be interpreted as reflecting fluctuations in strength or position, respectively.

To illustrate this coupling of strength and position fluctuations in the PC time series, 10^4 realizations of the field (1) with $h = w/\sigma_0 = 0.26$ were made for a range of values of $l = \gamma/U_0$ (selected such that $f_1(\phi)$ remains the leading EOF), and the time series $\alpha^{(1)}(t)$ and $\alpha^{(2)}(t)$ were calculated. Scatter plots of these time series are plotted in Figure 8, conditioned on the sign of $\xi(t)$ (dark for $\xi < 0$, light for $\xi > 0$). It is evident in Figure 8 that, for sufficiently weak fluctuations in jet strength, the distribution clusters around the parabolic curve associated with the projection of position fluctuations on both $E^{(1)}(\phi)$ and $E^{(2)}(\phi)$. It is also clear that both fluctuations in strength and position generally project along $E^{(2)}(\phi)$, precluding its interpretation in terms of either individually.

7 Dependent Fluctuations in Strength and Width

Consider now the case in which only fluctuations in position are zero (i.e. $\gamma \neq 0, w = 0$, $v \neq 0$), and where, as suggested by the observations, the fluctuations in strength and inverse width are correlated, i.e. $\xi(t) = \rho\eta(t)$. Then

$$u(\phi, t) = (U_0 + \rho\eta(t)) \exp\left(-\frac{(\phi - \phi_0)^2}{2\sigma_0^2}(1 + \eta(t))^2\right). \tag{46}$$

The time mean jet is:

$$\begin{aligned} \langle u(\phi)\rangle &= \int_{-\infty}^{\infty} \frac{1}{\sqrt{2\pi v^2}} \exp\left(-\frac{\eta^2}{2v^2}\right) u(\phi, t) \qquad (47) \\ &= \frac{\sigma_0}{\sqrt{\sigma_0^2 + v^2(\phi - \phi_0)^2}} \left(U_0 - \frac{\rho v^2(\phi - \phi_0)^2}{\sigma_0^2 + v^2(\phi - \phi_0)^2}\right) \exp\left(-\frac{1}{2}\frac{(\phi - \phi_0)^2}{\sigma_0^2 + v^2(\phi - \phi_0)^2}\right). \end{aligned}$$

As before, the mean jet is distinct from the instantaneous jet with mean width. Calculating the covariance function, we find that:

$$\begin{aligned} C(x,y) &= \frac{1}{\sqrt{(1+v^2x^2)(1+v^2y^2)}} \exp\left(-\frac{1}{2}\frac{x^2+y^2}{1+v^2(x^2+y^2)}\right) \times \\ &\left[\sqrt{1+\frac{v^4x^2y^2}{1+v^2(x^2+y^2)}}\left\{\left(U_0-\frac{\rho v^2(x^2+y^2)}{1+v^2(x^2+y^2)}\right)^2+\frac{\rho^2v^2}{1+v^2(x^2+y^2)}\right\}\right. \\ &\left.-\exp\left(-\frac{1}{2}\frac{v^2x^2y^2}{1+v^2(x^2+y^2)}\left[\frac{1}{1+v^2x^2}+\frac{1}{1+v^2y^2}\right]\right)\left(U_0-\frac{\rho v^2x^2}{1+v^2x^2}\right)\left(U_0-\frac{\rho v^2y^2}{1+v^2y^2}\right)\right], \end{aligned} \tag{48}$$

where x and y are defined as in Eqns (32) and (33). This function is not manifestly separable for general values of v, but for $v << 1$, we have:

$$C(x,y) = \frac{1}{\sqrt{(1+v^2x^2)(1+v^2y^2)}} \exp\left(-\frac{1}{2}\frac{x^2+y^2}{1+v^2(x^2+y^2)}\right)\left(v^2[\rho-U_0x^2][\rho-U_0y^2]+O(v^4)\right) \tag{49}$$

so

$$C(\phi_1,\phi_2) = \sqrt{\pi}\sigma_0U_0^2v^2\left[\left(\frac{\rho}{U_0}\right)^2-\left(\frac{\rho}{U_0}\right)+\frac{3}{4}\right]E^{(1)}(\phi_1)E^{(1)}(\phi_2)+O(v^4) \tag{50}$$

where

$$E^{(1)}(\phi) = \frac{1}{\sqrt{\frac{4}{3}\left(\frac{\rho}{U_0}\right)^2-\frac{4}{3}\left(\frac{\rho}{U_0}\right)+1}}[f_2(\phi)+\frac{2}{\sqrt{3}}\left(1-\frac{\rho}{U_0}\right)f_0(\phi)] \tag{51}$$

is the leading EOF for pure correlated fluctuations in jet strength and inverse width.

The mixing of the functions $f_0(\phi)$ and $f_2(\phi)$ in $E^{(1)}(\phi)$ depends on the ratio ρ/U_0; in particular, when this ratio is equal to 1, $E^{(1)}(\phi)$ is aligned along $f_2(\phi)$ (i.e. it is a tripole) and when the ratio is very large, $E^{(1)}(\phi)$ is approximately aligned along $f_0(\phi)$ (i.e. it is a monopole). Figure 9 displays plots of $E^{(1)}(\phi)$ for a representative range of the values of the ratio ρ/U_0.

8 Fluctuations in Strength, Position, and Width

In considering the general cases of fluctuations in both strength and width, or all three of strength, position, and width, direct calculation of the covariance matrix is mathematically

intractable. In the limiting cases considered in Sections 3 through 7, the leading EOFs lie in the 3-dimensional space spanned by $f_0(\phi), f_1(\phi)$, and $f_2(\phi)$. Motivated by these results, we proceed by assuming that (to a first approximation) the zonal mean zonal wind $u(\phi, t)$ can be expressed in terms of the basis vectors $f_0(\phi), f_1(\phi)$ and $f_2(\phi)$ alone:

$$u(\phi, t) = a_0(t) f_0(\phi) + a_1(t) f_1(\phi) + a_2(t) f_2(\phi). \tag{52}$$

We then consider the statistical structure of the zonal mean zonal wind projected into this 3-dimensional subspace.

Defining the projections of $u(\phi, t)$ on the basis vectors $f_i(\phi)$:

$$p_i(t) = \int_{-\infty}^{\infty} u(\phi, t) f_i(\phi) d\phi, \tag{53}$$

direct integration gives the following explicit forms:

$$p_0(t) = (2\sqrt{\pi}\sigma_0)^{1/2} Z(t) \tag{54}$$

$$p_1(t) = 2(\sqrt{\pi}\sigma_0)^{1/2} \frac{[1+\eta(t)]^2}{1+[1+\eta(t)]^2} \left(\frac{\lambda(t)}{\sigma_0}\right) Z(t) \tag{55}$$

$$p_2(t) = -2\left(\frac{2\sqrt{\pi}\sigma_0}{3}\right)^{1/2} \frac{[1+\eta(t)]^4 \left(1 - \left(\frac{\lambda(t)}{\sigma_0}\right)^2\right) + [1+\eta(t)]^2}{(1+[1+\eta(t)]^2)^2} Z(t) \tag{56}$$

where

$$Z(t) = \frac{U_0 + \xi(t)}{(1+[1+\eta(t)]^2)^{1/2}} \exp\left(-\frac{1}{2} \frac{[1+\eta(t)]^2}{1+[1+\eta(t)]^2} \left(\frac{\lambda(t)}{\sigma_0}\right)^2\right). \tag{57}$$

Because the vectors in the basis $(f_1(\phi), f_2(\phi), f_3(\phi))$ are not mutually orthogonal, the projection coefficients $p_i(t)$ will not equal the components $a_i(t)$ in Eq (52). In fact, the vector of components $\mathbf{a}(t)$ is related to the vector of projections $p(t)$ by:

$$\mathbf{a} = G^{-1}\mathbf{p} \tag{58}$$

where

$$G_{ij} = \int_{-\infty}^{\infty} f_i(\phi) f_j(\phi) d\phi \tag{59}$$

so

$$G^{-1} = \frac{1}{2}\begin{pmatrix} 3 & 0 & \sqrt{3} \\ 0 & 2 & 0 \\ \sqrt{3} & 0 & 3 \end{pmatrix}. \tag{60}$$

Denoting by $a_i'(t)$ the anomalies of the components $a_i'(t) = a_i(t) - \langle a_i(t)\rangle$ we can write the covariance matrix as:

$$C(\phi_1,\phi_2) = \left\langle (a_0')^2 \right\rangle f_0(\phi_1)f_0(\phi_2) + \left\langle (a_1')^2 \right\rangle f_1(\phi_1)f_1(\phi_2) \tag{61}$$

$$+ \left\langle (a_2')^2 \right\rangle f_2(\phi_1)f_2(\phi_2) + \langle a_0'a_2'\rangle \left[f_0(\phi_1)f_2(\phi_2) + f_2(\phi_1)f_0(\phi_2)\right], \tag{62}$$

where we have assumed that position fluctuations are uncorrelated with fluctuations in strength and inverse width (as suggested by the observations), so $\langle a_0'a_1'\rangle = \langle a_1'a_2'\rangle = 0$. Writing the eigenvector $E(\phi)$ over the basis set $f_i(\phi)$:

$$E(\phi) = b_0 f_0(\phi) + b_1 f_1(\phi) + b_2 f_2(\phi) \tag{63}$$

the integral equation for the eigenfunctions (67) can be expressed as

$$M\mathbf{b} = \mu\mathbf{b} \tag{64}$$

where

$$M = \begin{pmatrix} \langle (a_0')^2\rangle - \frac{1}{\sqrt{3}}\langle a_0'a_2'\rangle & 0 & -\frac{1}{\sqrt{3}}\langle (a_0')^2\rangle + \langle a_0'a_2'\rangle \\ 0 & \langle (a_1')^2\rangle & 0 \\ -\frac{1}{\sqrt{3}}\langle (a_2')^2\rangle + \langle a_0'a_2'\rangle & 0 & \langle (a_2')^2\rangle - \frac{1}{\sqrt{3}}\langle a_0'a_2'\rangle \end{pmatrix} \tag{65}$$

and $\mathbf{b} = (b_1, b_2, b_3)$. From this, we can read off the fact that $f_1(\phi)$ is an EOF with PC time series $a_1(t) = p_1(t)$ (as $\langle a_1\rangle = 0$ for symmetric fluctuations in λ). The other two EOFs are hybrids of $f_0(\phi)$ and $f_2(\phi)$, with components given by the solutions to the reduced eigenvalue problem

$$\begin{pmatrix} \langle (a_0')^2\rangle - \frac{1}{\sqrt{3}}\langle a_0'a_2'\rangle & -\frac{1}{\sqrt{3}}\langle (a_0')^2\rangle + \langle a_0'a_2'\rangle \\ -\frac{1}{\sqrt{3}}\langle (a_2')^2\rangle + \langle a_0'a_2'\rangle & \langle (a_2')^2\rangle - \frac{1}{\sqrt{3}}\langle a_0'a_2'\rangle \end{pmatrix} \begin{pmatrix} b_0 \\ b_2 \end{pmatrix} = \mu \begin{pmatrix} b_0 \\ b_2 \end{pmatrix}. \tag{66}$$

The ordering of these EOFs will depend on the details of the covariance structure of $\lambda(t), \eta(t)$, and $\xi(t)$. When restricted to this three-dimensional subspace, the dipole arises as an EOF of $u(\phi, t)$ even in the presence of simultaneous fluctuations in jet strength, width, and position. As was the case in the absence of fluctuations in width, while the PC time series associated with the dipole EOF represents fluctuations in jet position to leading order, there are higher order correction terms involving fluctuations in jet strength and width. Furthermore, while the PC time series will be uncorrelated, they will not be independent, as each will involve the time series of fluctuations in jet strength, position, and width. The dipole $f_1(\phi)$ clearly emerges as a privileged pattern in the set of leading EOFs, but one without a direct physical interpretation.

9 Discussion and Conclusions

This study has considered analytic calculations of the statistical structure of an idealised (yet physically motivated) midlatitude jet characterised by Gaussian fluctuations in its strength, position, and width. The following results were obtained.

- In general, the time mean jet does not equal the jet with time mean strength, width, and position. This difference implies an ambiguity in the definition of the jet climatology, although the difference is small for the parameters characteristic of the midlatitude troposphere.

- The leading EOF patterns of the fluctuating jet found in Wittman et al. (2005) were obtained analytically. To a first approximation, these EOFs can be described in terms of three elementary functions, $f_0(\phi), f_1(\phi)$, and $f_2(\phi)$ (Eqns. (11)-(13) and Figures 2 and 3), representing monopole, dipole, and tripole patterns respectively. The dipole is spatially orthogonal to the monopole and the tripole, so it arises naturally as an EOF if fluctuations in jet position are uncorrelated with fluctuations in strength and inverse

width. The monopole and tripole, however, are not orthogonal, so the remaining EOFs arise as linear combinations of these two structures. In particular, the EOF patterns for fluctuations in jet position or strength alone are not retained in the presence of fluctuations in both strength and position; these structures are mixed, or hybridised. Caution must therefore be exercised in interpreting a particular EOF pattern in terms of the EOFs produced by individual physical processes.

- The PC time series inextricably couple together the time series associated with the individual underlying physical processes. Individual EOF modes therefore cannot be associated in general with individual physical processes. The dipole EOF, which only occurs in the presence of fluctuations in jet position, has a corresponding PC time series which combines fluctuations in jet strength, position, and width. Although the strength and width fluctuations only come in as second order corrections to the PC time series, the dipole EOF mode does *not* simply correspond to fluctuations in jet position. The higher order EOFs cannot be simply interpreted (even to leading order) in terms of fluctuations in strength, width, or position. Note that the distinct physical processes in the PC time series cannot be decoupled through the selection of another basis set, such as would follow from a rotated EOF analysis. Furthermore, the dependence of each of the PC time series on all of the underlying processes implies that while these time series are uncorrelated, they are not independent (as is often assumed).

- The dipole pattern does arise naturally as an EOF of the fluctuating jet (although one without a straightforward physical interpretation), requiring only that fluctuations in jet position be uncorrelated with those in strength and inverse width. Angular momentum conservation, which was used in the model of Gerber and Vallis (2005), is not required to produce this structure.

The fluctuating jet considered in this study was idealised both in its meridional structure, and in the statistical structure of its fluctuations. In fact, observed jets are generally asymmetric about their peak and fluctuations in strength, position, and inverse width are generally non-Gaussian. A goal of future work is to investigate the effects on the jet covariance structure of jet asymmetries and non-Gaussian fluctuations.

The present study has therefore demonstrated, in the context of a fluctuating idealised zonal jet, that individual EOF modes cannot generally be associated with individual physical processes. This result, which is not surprising in light of the general study of North (1984), still stands in contrast to common practice (e.g. Feldstein and Lee, 1998; Feldstein, 2000; DeWeaver and Nigam, 2000; Vallis et al., 2004; Codron, 2005; Wittman et al., 2005). Empirical Orthogonal Function analysis is a powerful tool for dimensionality reduction in multivariate datasets, but it is a purely statistical operation. At times, it may be possible to interpret individual EOF modes in terms of underlying physical processes, but such interpretations should be approached with the utmost caution.

Acknowledgements

We would like to thank Slava Kharin and John Scinocca for their helpful comments on this manuscript. Adam Monahan acknowledges support from the Natural Sciences and Engineering Research Council of Canada and from the Canadian Institute for Advanced Research Earth System Evolution Program.

Appendix A: Calculating the EOFs

Consider the covariance function $C(\phi_1, \phi_2)$, defined as in Eq. (10). The EOFs $E^{(j)}(\phi)$ of $u(\phi)$ are then defined as solutions of the integral equation:

$$\int_{-\infty}^{\infty} C(\phi_1, \phi_2) E^{(j)}(\phi_2) = \mu^{(j)} E^{(j)}(\phi_1). \tag{67}$$

If the covariance matrix is separable, that is, if it can be expressed in the form:

$$C(\phi_1, \phi_2) = \sum_{i=1}^{N} \theta_i g_i(\phi_1) g_i(\phi_2), \tag{68}$$

for some linearly independent functions $g_i(\phi)$, $i = 1, ..., N$, then the integral equation can be reduced to the matrix equation:

$$\sum_{k=1}^{N} \theta_i G_{ik} a_k^{(j)} = \mu^{(j)} a_i^{(j)}, \tag{69}$$

where $a_i^{(j)}$ are the components of $E^{(j)}(\phi)$ over the basis $g_i(\phi)$:

$$E^{(j)}(\phi) = \sum_{i=1}^{N} a_i^{(j)} g_i(\phi) \tag{70}$$

and

$$G_{ik} = \int_{-\infty}^{\infty} g_i(\phi) g_k(\phi)\, d\phi. \tag{71}$$

Thus, if the covariance matrix is separable, the infinite dimensional integral equation for the EOFs can be reduced to a finite dimensional eigenvalue problem. In particular, if the functions $g_i(\phi)$ are mutually orthogonal, i.e., if $G_{jk} = \nu_j \delta_{ij}$, then the functions $g_i(\phi)$ are identical to the EOFs (up to a normalization factor).

For the covariance function (41) of Section 6, the integral equation (67) reduces to the problem of diagonalising a 3×3 matrix. As the vector $f_1(\phi)$ is orthogonal to both $f_0(\phi)$ and $f_2(\phi)$, it is an eigenvector of $C(\phi_1, \phi_2)$; the EOF problem is thus reduced to a 2×2 problem for the eigenvectors in the space spanned by $f_0(\phi)$ and $f_2(\phi)$:

$$\sqrt{\pi}\sigma_0 U_0^2 \begin{pmatrix} l^2 & -\frac{l^2}{\sqrt{3}} \\ -\frac{\sqrt{3}h^4}{8} & \frac{3h^4}{8} \end{pmatrix} \begin{pmatrix} \beta_0 \\ \beta_2 \end{pmatrix} = \mu \begin{pmatrix} \beta_0 \\ \beta_2 \end{pmatrix} \tag{72}$$

for which the eigenvalues (corresponding to the EOF variances) are

$$\mu^{(\pm)} = \frac{\sqrt{\pi}\sigma_0 U_0^2}{2}\left(l^2 + \frac{3h^4}{8} \pm \sqrt{\left(l^2 + \frac{3h^4}{8}\right)^2 - l^2 h^4}\right). \tag{73}$$

The components of the associated eigenvectors satisfy:

$$\beta_0^{(\pm)} = \frac{l^2}{\sqrt{3}\left[l^2 - \mu^{(\pm)}/(\sqrt{\pi}\sigma_0 U_0^2)\right]}\beta_2^{(\pm)} \tag{74}$$

with normalization constraint

$$(\beta_0^{(\pm)})^2 - \frac{2}{\sqrt{3}}\beta_0^{(\pm)}\beta_2^{(\pm)} + (\beta_2^{(\pm)})^2 = 1. \tag{75}$$

In the limit of that $l^2 << h^4$,

$$\mu^{(+)} \sim \sqrt{\pi}\sigma_0 U_0^2 \frac{3h^4}{8} \tag{76}$$

$$\mu^{(-)} \sim \frac{4}{3}\frac{\pi}{\sigma_0} U_0^2 l^2 \tag{77}$$

and $|\beta_0^{(+)}| << |\beta_2^{(+)}|$ while $|\beta_0^{(-)}|$ and $|\beta_2^{(-)}|$ are of the same order of magnitude. Conversely, in the limit that $l^2 >> h^4$,

$$\mu^{(+)} = \sqrt{\pi}\sigma_0 U_0^2 l^2 \tag{78}$$

$$\mu^{(-)} = \frac{\sqrt{\pi}\sigma_0 h^4}{8} \tag{79}$$

and $|\beta_0^{(+)}| >> |\beta_2^{(+)}|$ while $|\beta_0^{(-)}|$ and $|\beta_2^{(-)}|$ are of the same order of magnitude.

Thus, when jet strength fluctuations are relatively weak, the larger of the two EOFs spanned by $f_0(\phi)$ and $f_2(\phi)$ corresponds to the second EOF of the case with fluctuations in jet position alone, lying almost parallel to $f_2(\phi)$ and explaining exactly the correct amount of variance (c.f. Eq. (24)). When jet strength fluctuations are relatively strong, the larger of the two EOFs spanned by $f_0(\phi)$ and $f_2(\phi)$ corresponds to the leading EOF of the situation in which there are fluctuations in jet strength alone, also with the correct variance (c.f. Eq. (16)). In both limiting cases, the smaller of the two EOFs spanned by $f_0(\phi)$ and $f_2(\phi)$ is a mixture of both vectors. To leading order, in the limits of both weak and strong fluctuations in jet strength, the respective cases of fluctuations in jet position alone is recovered and in jet strength alone is recovered.

Appendix B: Gaussian Jet Fitting Procedure

Given the jet structure,

$$u(\phi) = U \exp\left(-\frac{(\phi - \Phi)^2}{2\sigma^2}\right) \tag{80}$$

we can take logarithms of both sides (over the latitude range where $u(\phi) > 0$) to obtain

$$\begin{aligned} \ln u &= \ln U - \frac{1}{2\sigma^2}(\phi - \Phi)^2 \\ &= \left(\ln U - \frac{\Phi^2}{2\sigma^2}\right) + \frac{\Phi}{\sigma^2}\phi - \frac{1}{2\sigma^2}\phi^2 \\ &= a_1 + a_2\phi + a_3\phi^2. \end{aligned} \tag{81}$$

Optimizing the parameters a_1, a_2, a_3 to minimise the squared misfit:

$$\epsilon^2 = \left(\ln u - a_1 - a_2\phi - a_3\phi^2\right)^2 \tag{82}$$

is a simple multiple linear regression problem which can be expressed:

$$\begin{pmatrix} \langle \ln u \rangle \\ \langle \phi \ln u \rangle \\ \langle \phi^2 \ln u \rangle \end{pmatrix} = \begin{pmatrix} 1 & \langle \phi \rangle & \langle \phi^2 \rangle \\ \langle \phi \rangle & \langle \phi^2 \rangle & \langle \phi^3 \rangle \\ \langle \phi^2 \rangle & \langle \phi^3 \rangle & \langle \phi^4 \rangle \end{pmatrix} \begin{pmatrix} a_1 \\ a_2 \\ a_3 \end{pmatrix} \tag{83}$$

where $\langle \cdot \rangle$ denotes the spatial average over the range of latitudes used for the fitting. Writing this equation as $\mathbf{Y} = M\mathbf{X}$ we solve for the vector $\mathbf{X} = (a_1, a_2, a_3)$ as $\mathbf{X} = M^{-1}\mathbf{Y}$. From this, we obtain:

$$\sigma = \sqrt{-\frac{1}{2a_3}} \tag{84}$$

$$\Phi = -\frac{a_2}{2a_3} \tag{85}$$

$$U = \exp\left(a_1 - \frac{a_2^2}{4a_3}\right). \tag{86}$$

References

Ambaum, M. H., B. J. Hoskins, and D. B. Stephenson, 2001: Arctic Oscillation or North Atlantic Oscillation? *J. Climate*, **14**, 3495–3507.

Arfken, G., 1985: *Mathematical Methods for Physicists*. Academic Press, San Diego, 985 pp.

Barnston, A. G. and R. E. Livezey, 1987: Classification, seasonality, and persistence of low-frequency atmospheric circulation patterns. *Mon. Wea. Rev.*, **115**, 1083–1126.

Codron, F., 2005: Relation between annular modes and the mean state: Southern Hemisphere summer. *J. Climate*, **18**, 320–330.

DeWeaver, E. and S. Nigam, 2000: Do stationary waves drive the zonal-mean jet anomalies of the northern winter? *J. Climate*, **13**, 2160–2176.

Dommenget, D. and M. Latif, 2002: A cautionary note on the interpretation of EOFs. *J. Climate*, **15**, 216–225.

Farrell, B. F. and P. J. Ioannou, 1996: Generalized stability theory. Part I: autonomous operators. *J. Atmos. Sci.*, **53**, 2025–2040.

Feldstein, S. and S. Lee, 1998: Is the atmospheric zonal index driven by an eddy feedback? *J. Atmos. Sci.*, **55**, 3077–3086.

Feldstein, S. B., 2000: Is interannual zonal mean flow variability simply climate noise? *J. Clim.*, **13**, 2356–2362.

Fyfe, J. C., 2003: Separating extratropical zonal wind variability and mean change. *J. Climate*, **16**, 863–874.

Fyfe, J. C. and D. J. Lorenz, 2005: Characterizing zonal wind variability: Lessons from a simple GCM. *J. Climate*, **18**, 3400–3404.

Gerber, E. P. and G. K. Vallis, 2005: A stochastic model for the spatial structure of annular patterns of variability and the North Atlantic Oscillation. *J. Climate*, **18**, 2102–2118.

Gill, A. E., 1982: *Atmosphere-Ocean Dynamics*. Academic Press, San Diego, 662 pp.

Monahan, A. H., J. C. Fyfe, and L. Pandolfo, 2003: The vertical structure of wintertime climate regimes of the Northern Hemisphere extratropical atmosphere. *J. Climate*, **16**, 2005–2021.

North, G. R., 1984: Empirical orthogonal functions and normal modes. *J. Atmos. Sci.*, **41**, 879–887.

Palmer, T. N., 1999: A nonlinear dynamical perspective on climate prediction. *J. Climate*, **12**, 575–591.

Penland, C., 1996: A stochastic model of IndoPacific sea surface temperature anomalies. *Physica D*, **98**, 534–558.

Thompson, D. W. and J. M. Wallace, 2000: Annular modes in the extratropical circulation part I: Month-to-month variability. *J. Climate*, **13**, 1000–1016.

Vallis, G. K., E. P. Gerber, P. J. Kushner, and B. A. Cash, 2004: A mechanism and simple dynamical model of the North Atlantic Oscillation and annular modes. *J. Atmos. Sci.*, **61**, 264–280.

Wittman, M. A., A. J. Charlton, and L. M. Polvani, 2005: On the meridional structure of annular modes. *J. Climate*, **18**, 2199–2122.

Figure Captions

Figure 1: Leading EOFs of daily Southern Hemisphere winter (May-Sep) 500 hPa zonal mean zonal wind (1958-2003). Top: Following the fitting procedure in accord with Eqns (1)-(7). Bottom: Not following the fitting procedure. Solid curves: $E^{(1)}$. Dashed curves: $E^{(2)}$.

Figure 2: *Dramatis Personae*: Plots of the functions $f_0(\phi)$, $f_1(\phi)$, and $f_2(\phi)$ (Eqns. (11)-(13)) from which the leading EOFs are constructed, rescaled to be of unit norm.

Figure 3: Geometric illustration of the vectors (in function space) $f_0(\phi)$, $f_1(\phi)$, and $f_2(\phi)$. Because $f_0(\phi)$ and $f_2(\phi)$ are not orthogonal, they cannot simultaneously be eigenvectors of a symmetric function such as the covariance. If both of these vectors contribute to the leading EOFs, these EOFs must be orthogonal linear combinations of these vectors.

Figure 4: Leading EOF of pure Gaussian fluctuations in jet width (Eq. 36). Normalization as in Figure 2.

Figure 5: The orientations in the space spanned by $f_0(\phi), f_1(\phi), f_2(\phi)$ of the leading EOFs for the cases of pure fluctuations in jet strength, position, and width.

Figure 6: Components of the EOFs spanned by $f_0(\phi)$ and $f_2(\phi)$ for fluctuations in both jet strength and position, (a) for the EOF with the larger variance $\mu^{(+)}$, and (b) for the EOF with the smaller variance $\mu^{(-)}$.

Figure 7: Hybrid EOFs $\mathrm{E}^{(+)}$ of the covariance function (41) for values of the ratio $3h^4/8l^2$ equal to 0.3 (thin solid curve), 1 (thick curve), and 3 (dashed curve).

Figure 8: Scatter plots of numerically calculated $\alpha^{(1)}(t)/U_0$ vs. $\alpha^{(2)}(t)/U_0$ for $h = 0.26$ and $3h^4/8l^2 = 0.1, 0.25, 1, 2.5$, and 10. Dark dots denote those points for which $\xi < 0$, light dots those points for which $\xi > 0$.

Figure 9: Leading EOF in case of correlated strength and inverse width fluctuations, for $\rho/U_0 = 0.01$ (thin solid line), $\rho/U_0 = 1$ (thick solid line), and $\rho/U_0 = 100$ (dashed line).

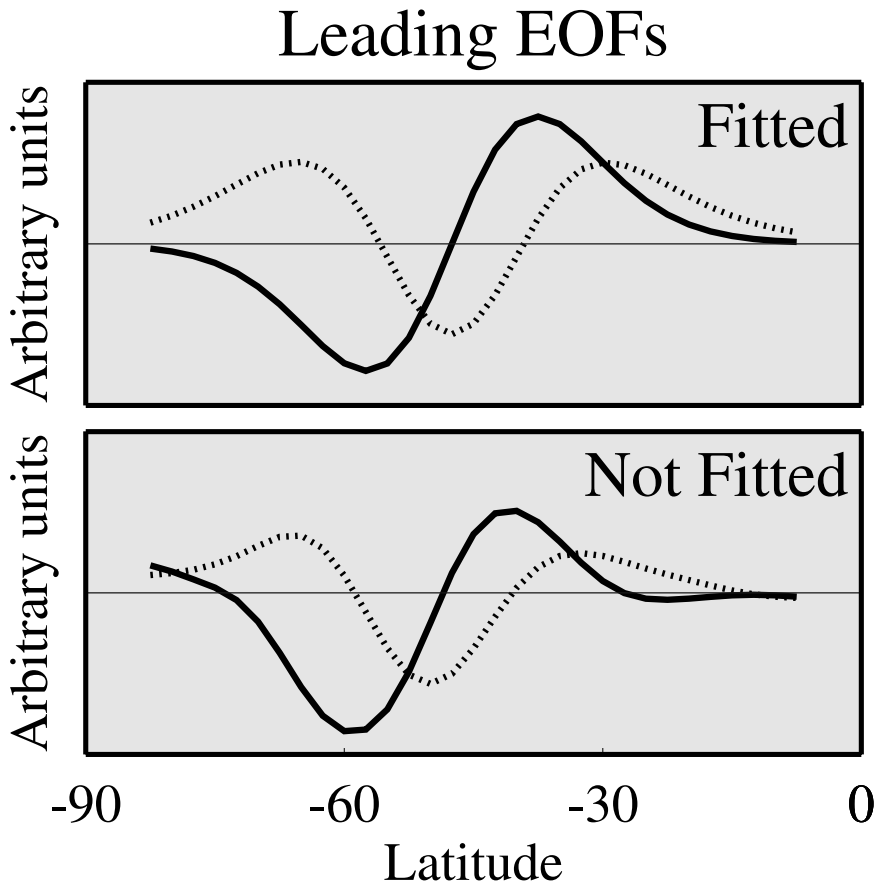

Figure 1: Leading EOFs of daily Southern Hemisphere winter (May-Sep) 500 hPa zonal mean zonal wind (1958-2003). Top: Following the fitting procedure in accord with Eqns (1)-(7). Bottom: Not following the fitting procedure. Solid curves: $E^{(1)}$. Dashed curves: $E^{(2)}$.

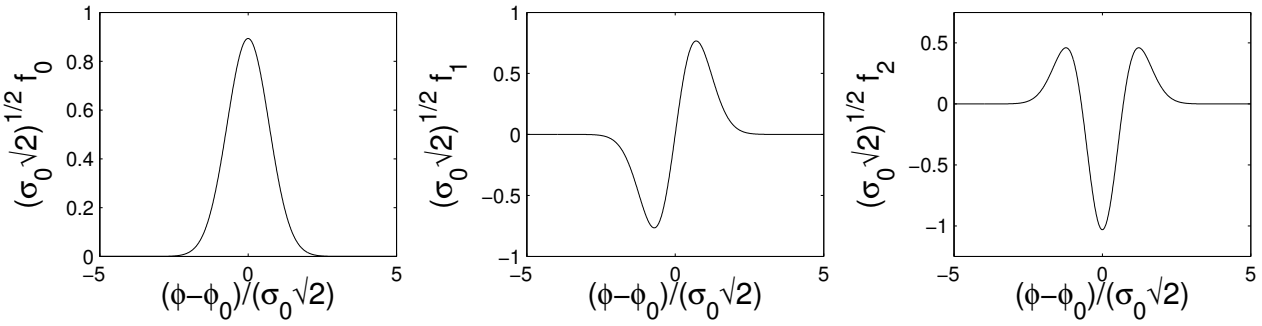

Figure 2: *Dramatis Personae*: Plots of the functions $f_0(\phi)$, $f_1(\phi)$, and $f_2(\phi)$ (Eqns. (11)-(13)) from which the leading EOFs are constructed, rescaled to be of unit norm.

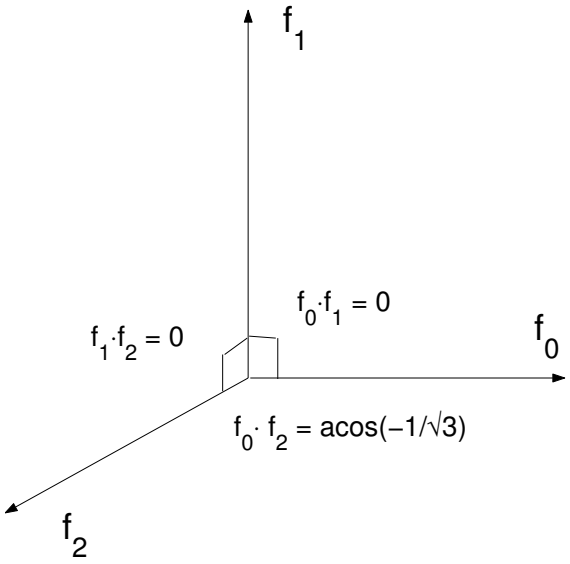

Figure 3: Geometric illustration of the vectors (in function space) $f_0(\phi)$, $f_1(\phi)$, and $f_2(\phi)$. Because $f_0(\phi)$ and $f_2(\phi)$ are not orthogonal, they cannot simultaneously be eigenvectors of a symmetric function such as the covariance. If both of these vectors contribute to the leading EOFs, these EOFs must be orthogonal linear combinations of these vectors.

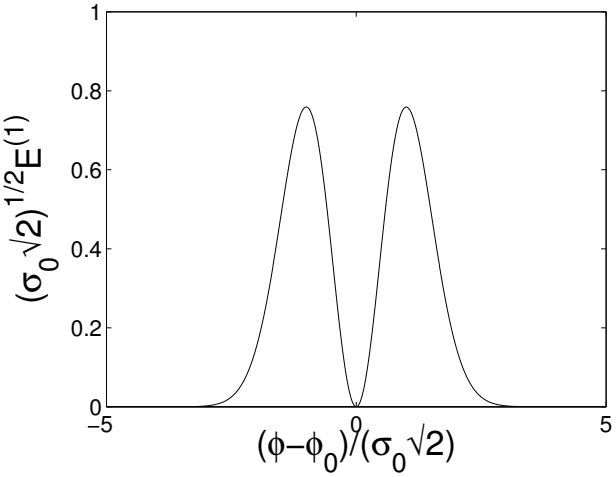

Figure 4: Leading EOF of pure Gaussian fluctuations in jet width (Eq. 36). Normalization as in Figure 2.

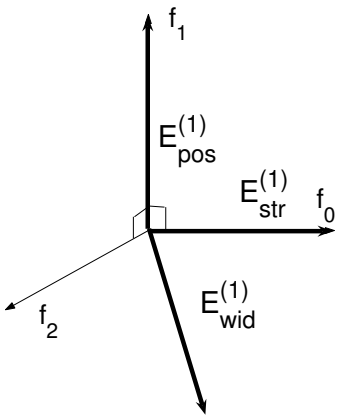

Figure 5: The orientations in the space spanned by $f_0(\phi), f_1(\phi), f_2(\phi)$ of the leading EOFs for the cases of pure fluctuations in jet strength, position, and width.

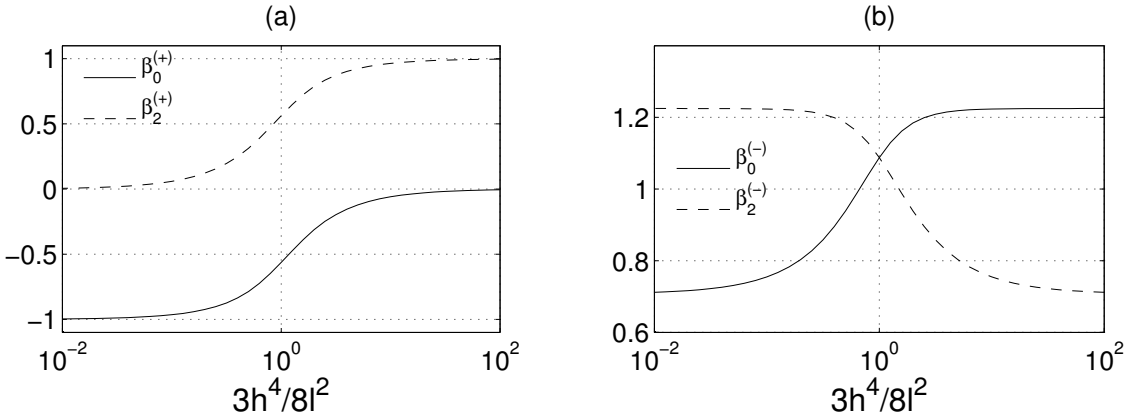

Figure 6: Components of the EOFs spanned by $f_0(\phi)$ and $f_2(\phi)$ for fluctuations in both jet strength and position, (a) for the EOF with the larger variance $\mu^{(+)}$, and (b) for the EOF with the smaller variance $\mu^{(-)}$.

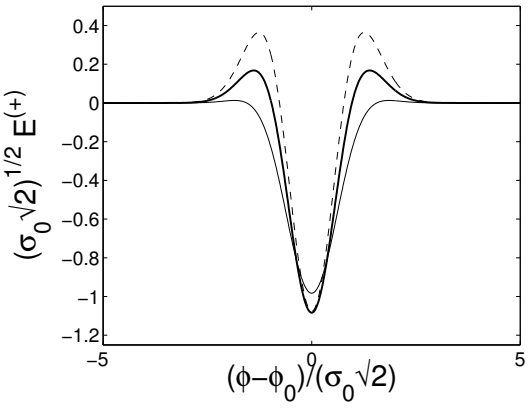

Figure 7: Hybrid EOFs $\mathrm{E}^{(+)}$ of the covariance function (41) for values of the ratio $3h^4/8l^2$ equal to 0.3 (thin solid curve), 1 (thick curve), and 3 (dashed curve).

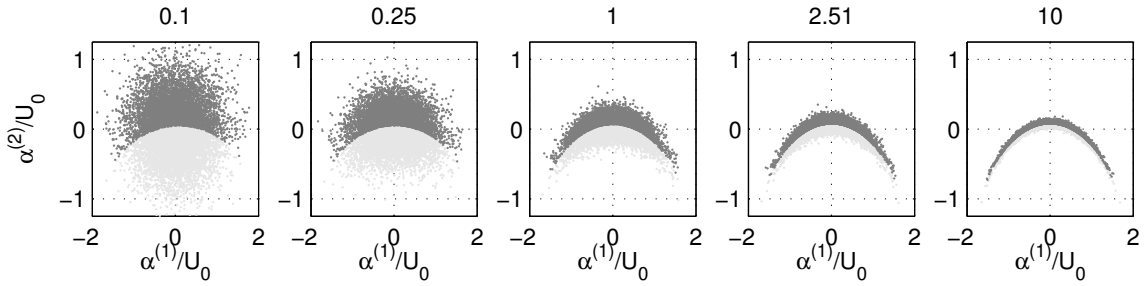

Figure 8: Scatter plots of numerically calculated $\alpha^{(1)}(t)/U_0$ vs. $\alpha^{(2)}(t)/U_0$ for $h = 0.26$ and $3h^4/8l^2 = 0.1, 0.25, 1, 2.5$, and 10. Dark dots denote those points for which $\xi < 0$, light dots those points for which $\xi > 0$.

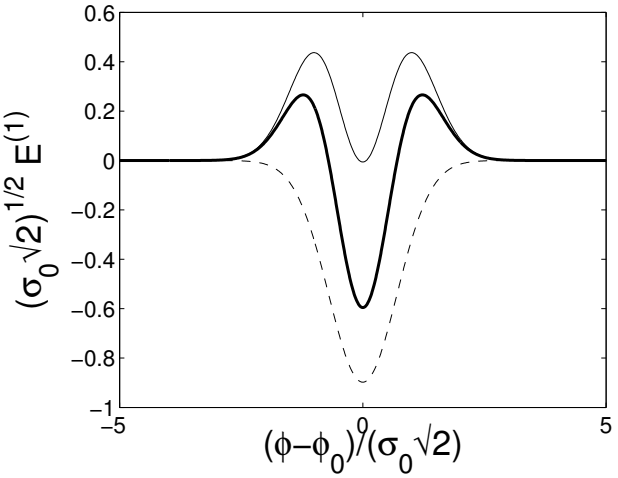

Figure 9: Leading EOF in case of correlated strength and inverse width fluctuations, for $\rho/U_0 = 0.01$ (thin solid line), $\rho/U_0 = 1$ (thick solid line), and $\rho/U_0 = 100$ (dashed line).